Received: 10 May 2024 | Revised: 23 July 2024 | Accepted: 26 August 2024

DOI: 10.1002/pol.20240377

RESEARCH ARTICLE

JOURNAL OF POLYMER SCIENCE WILEY

Preparation of poly(3-hexylthiophene) conjugated polymer brush films from amine-terminated surfaces

Olivia J. Armendarez[1] | **Grace C. Parizek**[1] | **Ruth J. Augustine**[1] | **Evan J. Silver**[1] | **Tristan A. Kaz**[1] | **Kaylee A. Campbell**[1] | **Isabella P. Diaz**[1] | **Shobha Mantripragada**[2] | **Robert D. Geil**[3] | **Sadie M. Flagg**[1] | **Brian H. Augustine**[1,4] | **Pamela M. Lundin**[1]

[1]Department of Chemistry, High Point University, High Point, North Carolina, USA

[2]Department of Nanoengineering, Joint School of Nanoscience and Nanoengineering, North Carolina A&T State University, Greensboro, North Carolina, USA

[3]Department of Chemistry, Chapel Hill Analytical and Nanofabrication Laboratory, University of North Carolina, Chapel Hill, North Carolina, USA

[4]Department of Chemistry, Furman University, Greenville, South Carolina, USA

Correspondence
Brian H. Augustine and Pamela M. Lundin, Department of Chemistry, High Point University, High Point, NC 27268, USA.
Email: brian.augustine@furman.edu and plundin@highpoint.edu

Funding information
Division of Chemistry, Grant/Award Number: 1919685; Division of Materials Research, Grant/Award Number: 2320222; North Carolina Biotechnology Center, Grant/Award Number: 2023-FLG-0025; National Nanotechnology Coordinating Office, Grant/Award Numbers: ECCS-20254P62, ECCS-2025064

Abstract

Conjugated polymer brush (CPB) films are more robust and exhibit more vertically aligned polymer chains than their spun-cast analogs. We prepare CPB films of poly(3-hexylthiophene) (P3HT) by coupling an amine-terminated surface (ATS) formed from (3-aminopropyl)triethoxysilane (APTES) on Si/SiO_2 to 4-bromobenzoic acid using standard, inexpensive peptide coupling reagents. The resulting terminal bromobenzene is reacted with $Pd(PtBu_3)_2$ and immersed in the monomer solution. X-ray photoelectron spectroscopy, spectroscopic ellipsometry and static water contact angle measurements confirm the surface chemistry at each stage of P3HT CPB preparation. Atomic force microscopy(AFM) and UV–vis spectrophotometry indicate that the CPB films prepared by this method exhibit similar morphology and optical properties to those produced from other methods of poly(3-alkylthiophene) CPB film preparation. Variations of the standard approach, such as using a pre-synthesized silane counterpart or with (11-aminoundecyl)triethoxysilane, show comparable film morphologies by AFM. This method is used to produce the first CPB film of poly(3-dodecylthiophene), showing its utility for exploring CPB films of more sterically demanding polymers. Peptide coupling is used to prepare an analogous functionalized thiol for initiating P3HT CPB film growth from Au surfaces, and microcontact printing with this thiol allows preparation of the first patterned CPB film of P3HT.

KEYWORDS

(3-aminopropyl)triethoxysilane, conjugated polymer brush films, microcontact printing, poly (3-hexylthiophene)

1 | INTRODUCTION

Conjugated polymer brush (CPB) films are materials in which the conjugated polymer chain is covalently bonded to a substrate, resulting in a polymer chain whose orientation with respect to the surface is more vertical than spun-cast conjugated polymer films.[1] The higher anisotropy of these films result in improved properties such as lower electrical resistivity[1] and higher thermal conductivity,[2] which are attractive properties for the next generation of organic electronic devices. The covalent nature of the surface attachment creates a more ordered and robust film[3] that leads to improved performance as a hole-transport layer in a polymer solar cell[4] and higher interfacial resistance leading to larger intrachain carrier mobility in an organic spin valve device.[5] CPBs have been successfully prepared from nanosurfaces such as carbon nanotubes,[6] silica nanospheres and nanocrystals,[7,8] gold nanoparticles,[9] and dispersed reduced graphene oxide.[10] Finer vibronic structure is observed versus the solution-phase polymer counterpart on the nanotubes, which is reflective of a high degree of order and planarization of the polymer on the surface.[6]

To achieve high grafting density and overall film quality, a grafting-from approach, in which polymerization is initiated from a functionalized surface and continued by a chain-growth mechanism, is preferred for CPB films. The π-system along the backbone lends itself to a cross-coupling approach known as catalyst-transfer polycondensation (CTP) in which the metal catalyst coordinates to the π-electron system and "chain walks" to the end of the chain to oxidatively insert into the aryl halide moiety, regenerating the initiator and re-starting the process to add another monomer.[11] To initiate the CTP, the surface is functionalized by the catalytic initiator, typically Ni or Pd, by oxidative addition of the metal into an aryl bromide or iodide anchored to the surface. The arene can be a benzene or thiophene, and in some cases an ortho-methyl substituent is present due to evidence in the solution-phase CTP literature that it helps initiate polymer growth.[12] The initiating arene is typically grafted to the surface through a self-assembled monolayer (SAM) or a surface that has been chemically functionalized.

Despite the promise of CPB films for applications in organic electronics, to date there are only a handful of reports on their preparation on large planar substrates such as indium tin oxide[1,13–15] silicon oxide,[13,16] and gold.[13,17] The surface functionalization strategies used typically hold the Ni or Pd initiating complex close to the surface, with the arene ligand being either directly attached to the surface[3,16] or separated by a single carbon (a benzyl moiety).[14,18] Surface functionalization with longer alkyl tethers require either multistep synthesis[13,19] or are limited to specialized chemicals that can be purchased.[2] As a result, studies on how the underlying surface chemistry influences the CPB film properties are limited.

To fill this gap, we have devised a straightforward method of preparing chemically functionalized surfaces capable of CTP initiation by using standard peptide coupling reagents to modify the terminal amine moiety of aminoalkylsilanes, such as (3-aminopropyl)triethoxysilane (APTES), on SiO_2 with 4-bromobenzoic acid, all of which are commercially available precursors (Scheme 1). Amine-terminated surfaces (hereafter referred to as ATS) such as APTES have long been used as a starting point for building more complex engineered surfaces including polymer brushes.[20–24] The peptide coupling used in this method can be performed directly on an ATS (ATS-first approach, Scheme 1 blue box), which can simplify purification, or prior to surface functionalization (synthesis-first approach, Scheme 1 gold box), which can be better in cases where the preparation of an ATS such as that of 2-aminoethanethiol on Au is less straightforward than that of APTES on Si/SiO_2. It should be noted that the term self-assembled monolayer (SAM) is often used in the literature to describe similar surface treatments, but as described by Xia et al., true SAMs have specific requirements of being high density 2-D quasicrystalline molecular layers which tend to be self-healing and defect-rejecting.[25] Surfaces modified by APTES and similar molecules, while often called SAMs in the literature, do not meet the definition of self-assembly since the surface is not self-limiting and is not well-ordered.[26,27] In this report, x-ray photoelectron spectroscopy (XPS), spectroscopic ellipsometry (SE), and static water contact angle measurements are used to confirm the structures of all stages of CPB film preparation for the well-studied benchmark[28–30] conjugated polymer poly(3-hexylthiophene) (P3HT). Atomic force microscopy (AFM) indicates that variations of this preparation, such as pre-synthesizing the silane surface functionalization precursor or using commercially available aminoalkylsilane with a longer alkyl tether, does not significantly impact the resulting polymer film morphology. While we focus most of our studies on P3HT grown from SiO_2 surfaces, we show the versatility of our method for other surfaces by using an analogous thiol ATS on an Au surface prepared using the synthesis-first approach. We additionally utilize this thiol in microcontact printing (μCP) to produce a patterned CPB film of P3HT, which is the first such example of a patterned P3HT CPB film and to our knowledge, only the second example of a patterned CPB films overall,[3] and which illustrates the potential of this technique for creating more complex CPB film architectures on planar surfaces.

Interestingly, in contrast to most reports on CPB films, our surface preparation method allows us to grow P3HT

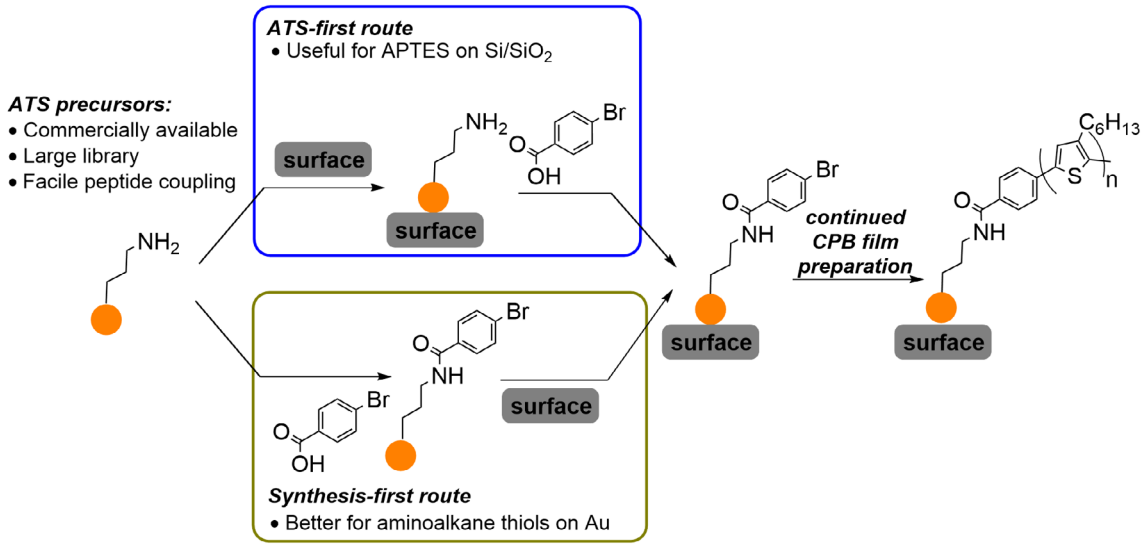

SCHEME 1 Use of amine-terminated surfaces in the preparation of poly(3-hexylthiophene) (P3HT) conjugated polymer brush (CPB) films through an amine-terminated surface (ATS)-first route (blue box), which has advantages for using (3-aminopropyl)triethoxysilane (APTES) on Si/SiO_2 surfaces, and a synthesis-first route (gold box), which gives better results in using aminoalkane thiols on Au surfaces.

CPB films as well as the even more sterically demanding poly(3-dodecylthiophene) (P3DDT). The majority of reports on CPB films grow poly(3-methylthiophene) (P3MT) or polythiophene (PT) rather than P3HT, which is justified for two reasons. First, because the CPB film is grown directly from the surface, rather than being deposited from solution, the bulky solubilizing hexyl group of P3HT is not needed. However, a second reason that the CPB film literature is dominated by P3MT and PT is that the steric bulk of the hexyl group of P3HT has been found to prevent efficient polymerization in the film state.[15,17,31] The two reports that did grow a P3HT CPB film on a large planar surface used a cross-linked poly(3-bromostyrene) film to initiate polymer growth,[16,32] rather than a direct treatment of the surface itself. Consequently, head-to-head comparisons of CPB films to conjugated polymer films formed from more traditional methods such as spin-casting, have been precluded. Therefore, our methodology, which allows the growth of CPB films of more sterically demanding but organic solvent-soluble polymers could provide a path forward not only for such studies, but also for the preparation of even more complicated conjugated polymer structures in the future.

2 | RESULTS AND DISCUSSION

2.1 | Synthesis of P3HT CPB films onto SiO_2 substrates

Preparation of the P3HT CPB films on oxidized silicon wafers began by the preparation of the ATS by immersion of O_2 plasma cleaned oxidized silicon wafers into a 2% v/v solution of the APTES in acetone (Scheme 2). Static deionized water contact angles of APTES terminated surfaces were used to confirm surface functionalization, with average values of 56.1° ± 2.0° increasing from 4.2° ± 0.9° for the plasma cleaned SiO_2 substrates (Tables S1 and S2 have complete contact angle data). The ATS was then further functionalized with a terminal bromobenzene group (**4BB SAM**) by coupling the terminal amine of the APTES-derived surface to 4-bromobenzoic acid using the standard peptide coupling reagent *N*-(3-dimethylaminopropyl)-*N*′-ethylcarbodiimide hydrochloride (EDC·HCl), along with catalytic 4-dimethylaminopyridine (DMAP). Contact angle measurements indicate that amide coupling happens quite quickly, with water contact angles of ∼80° after 15 min. To ensure high-quality functionalized surfaces, we left them in solution overnight to give average contact water angles of 81.0° ± 1.6°.

The **4BB SAM** was then functionalized with the catalytic initiator. Similar to the reports of others,[1,2] we found that surfaces functionalized with Ni initiators were capable of initiating polymer growth but the films formed were not conformal, with some regions showing thick polymer films and some regions showing no polymer at all. We suspect that this behavior may be due to increased reactivity of the Ni catalysts both in the polymerization and in undesirable side reactions that terminate polymer growth such as catalyst disproportionation. Films functionalized with palladium initiators provided much more reproducible results, and our ATSs were functionalized with Pd by submersion of the substrates in a solution of $Pd(P\textit{t}\text{-}Bu_3)_2$ in toluene. Water contact angles were not obtained for this step due to concerns regarding the stability of the Pd species in direct contact with water.

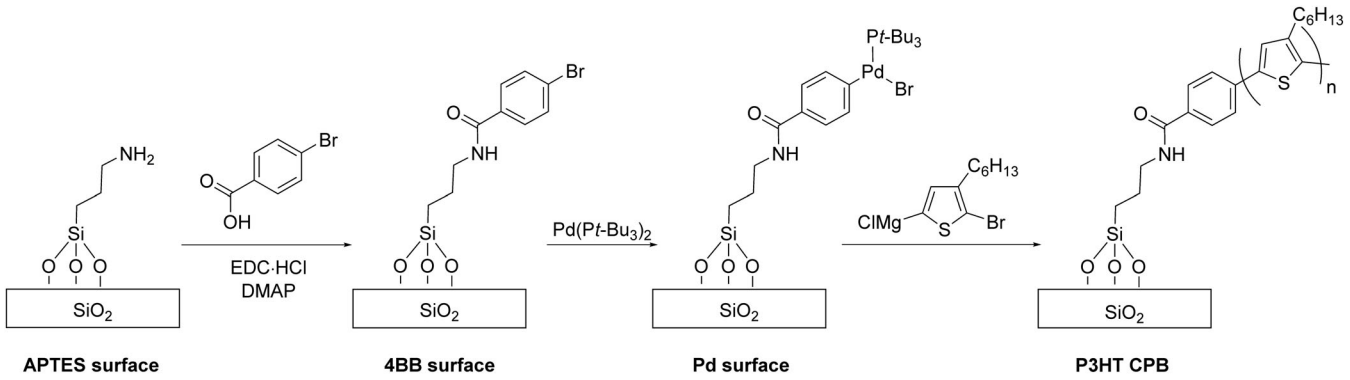

SCHEME 2 Amine-terminated functionalization and polymerization to produce poly(3-hexylthiophene) (P3HT) conjugated polymer brush (CPB) films on Si/SiO_2 using the amine-terminated surface (ATS)-first approach.

The monomer for polymerization of P3HT is generated in situ by a magnesium-iodine exchange between the 2-bromo-3-hexyl-5-iodothiophene and a commercially purchased solution of the Grignard reagent isopropylmagnesium chloride (iPrMgCl). Monomer addition to the growing polymer chain in the CTP mechanism involves a terminal thiophene bromide into which the initiator oxidatively inserts and then couples with the Grignard-functionalized end of the next monomer. Therefore, optimal polymerization efficiency of this AB-type polymerization relies on a clean exchange reaction at the 5-iodo position of the monomer precursor with minimal bismagnesiothiophene byproduct formed, because the incorporation of such a species into the growing chain would be incapable of continuing the CTP cycle. On the other hand, chain length in chain-growth mechanisms such as CTP are proportional to the [monomer]:[initiator] ratio so it is also desirable to convert as much as the monomer precursor into the active monomer as possible. Because it is common for commercial Grignard concentrations to deviate from the value indicated on the bottle, we have found that titration of the Grignard solution immediately prior to monomer formation is imperative. While many titration procedures for alkyl Grignard reagents are available, in our hands we obtained the best results using I_2 in a solution of LiCl in THF.[33] We used a volume of iPrMgCl solution that ensured that the amount added fell into a window of 0.95–1.00 stoichiometric equivalents with the monomer precursor. After monomer generation, our Pd-functionalized substrates were immersed in the monomer solution for 22 h to allow full polymerization.

2.2 | X-ray photoelectron spectroscopy

In order to confirm that each step shown in Scheme 2 was successfully accomplished on an oxidized Si substrate, we performed XPS with samples removed after each reaction step. Figure 1A shows XPS survey scan data from 0 to 700 eV normalized to the O 1s peak for each of the five reaction steps using oxidized Si substrates, from plasma-cleaned thermal SiO_2 to the P3HT CPB film. XPS is an ideal spectroscopic technique to monitor these sequential reaction steps because there should be a unique surface chemical signature after each successive reaction. The bottom (black spectrum) XPS survey scan is for the unfunctionalized ~100 nm thermally oxidized SiO_2 film on a Si wafer and thus the only elements observed should be due to Si and O which occur at binding energies of 102.3 and 531.7 eV for the Si 2p and O 1s signals, respectively (high resolution elemental XPS scans for each element reported are available in Figures S5–S11. Atomic percentages for each element are reported in Table 1). After the APTES deposition (red spectrum in Figure 1A), there are new peaks at binding energies of 399.1 and 284.9 eV for the N 1s and C 1s peaks, respectively, in addition to the substrate Si and O peaks.

The XPS spectrum of the **4BB SAM**, created by formation of an amide between the terminal amine of the APTES functionalized surface and 4-bromobenzoic acid, shows peaks due to the terminal Br at binding energies of 70.2 eV (Br 3d) and 256 eV (Br 3s), shown in the purple spectrum in Figure 1A. High resolution XPS shows that the C 1s peak (Figure 1B) is broader compared to the APTES terminated surface (Figure S5.c) with peaks fitted at 284.8 eV (35.0% of peak area), 285.7 eV (28.8% of peak area), 286.7 eV (18.6% of peak area) and 287.9 eV (16.7% of peak area). These binding energies correspond to C—C bonding in the APTES hydrocarbon chain and the benzene ring, the C—Br bond, the C—N bond, and the C═O bond of the amide, respectively. The O 1s peak also has a small shoulder at 533.7 eV (9.83% of peak area) due to the C═O bonding in the amide linker (see Figure S6.f) in addition to the SiO_2 bonding from the substrate and the silane bonds of the APTES at 531.1 eV.

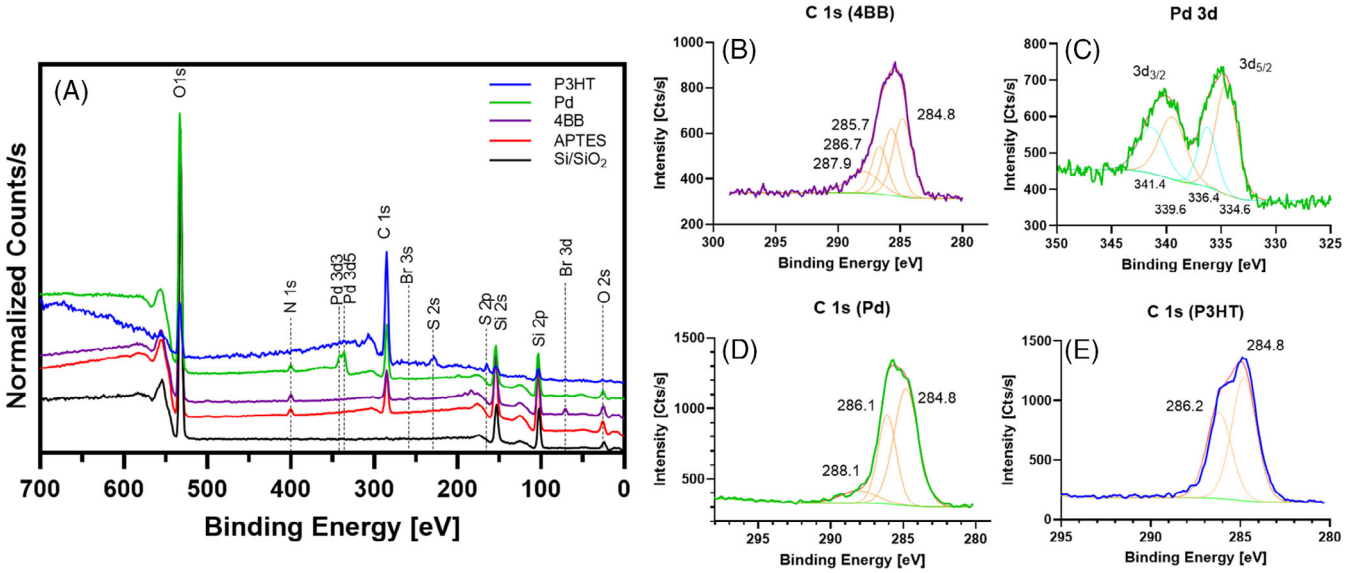

FIGURE 1 (A) X-ray photoelectron spectroscopy (XPS) survey scan from 0 to 700 eV of O_2 plasma-cleaned Si/SiO_2 substrate (black), (3-aminopropyl)triethoxysilane (APTES) treated Si/SiO_2 (red), 4BB terminated (purple), Pd treated 4BB film (green), P3HT CTP film (blue). Survey spectra were normalized to the O 1s peak and charge compensated to the C 1s peak at 284.8 eV; (B) C 1s scan from the 4BB sample. (C) Pd 3d scan from the Pd insertion step. (D) C 1s scan from the Pd insertion step. (E) C 1s scan of the P3HT film. High resolution XPS spectra colors correspond to survey scan colors.

TABLE 1 X-ray photoelectron spectroscopy (XPS) elemental atomic percentages as measured by XPS of each reaction layer starting with SiO_2 substrate.

	Surface termination layer				
Element	**SiO_2**	**ATPES**	**4BB**	**Pd**	**P3HT**
Br 3d	–	–	0.65	0.24	–
Si 2p	27.77	30.44	23.87	22.41	8.53
S 2p	–	–	–	–	2.51
C 1s	1.05	18.31	12.62	29.22	73.27
Pd 3d 5/2	–	–	–	0.99	–
N 1s	–	1.66	2.16	2.16	0.73
O 1s	72.18	49.59	60.71	44.46	14.97

The green spectrum in Figure 1A is from the Pd insertion step, showing a Pd doublet at ~335 and ~340 eV from Pd 3d 5/2 and 3d 3/2 electrons, respectively, shown in high resolution XPS in Figure 1C. The Pd 3d peaks have been fitted with four peaks at binding energies of 334.6 eV (37.8% of peak area), 336.4 eV (17.0% of peak area) for the 3d 5/2 peak, and 339.6 eV (25.7% of peak area) and 341.4 eV (19.5% of peak area) for the 3d 3/2 peak. Prior literature on an analogous Pd catalyzed P3MT CPB polymerization has reported that the two peaks are due to palladium atoms in Pd^0 and Pd^{II} oxidation states.[15] The authors were unable to identify the exact species of these peaks due to the complexity of the chemical environment of the Pd atom in the terminal complex. The Pd^0 peaks at ~334 and 340 eV are consistent with expected phosphine ligand backbonding to form the Pd—P dative bond. Another possibility is the existence of physisorbed Pd species due to disproportionation during the initiation reaction, which was not completely removed by rinsing. The XPS signal for Pd^{II} at ~336 and 341 eV would be consistent with the presence of both Pd-C and Pd-Br bonding found in the Pd complex. Unfortunately, this is also the expected binding energy which would result in the possible partial oxidation of the Pd—Br bond to form Pd—O in transferring the samples from the glovebox to the XPS instrument. Because of the existence of several unique Pd bonds in two oxidation states, and the possibility of the Pd—O bond, we cannot definitively assign the species responsible for the Pd 3d peaks but note that the peaks are consistent with the expected bonding on the surface and prior literature.[15] Figure 1D shows the C 1s spectrum of the Pd catalyst surface fitted with three peaks at binding energies of 284.8 eV (61.8% of peak area), 286.1 eV (33.9% of peak area) and 287.5 eV (4.3% of peak area). These binding energies are consistent with C—C bonding in the aromatic ring, APTES hydrocarbon chain and *t*-Bu_3 carbons at the surface, the C—P, C—N and C—Pd bonds, and the C═O bond in the amide, respectively. The intensity of the Br signal decreases after Pd insertion; this may imply that the Pd-functionalized headgroups of the surface may undergo disproportionation,[15] though the partial oxidation due to transferring the sample

to the XPS instrument as discussed above may also result in this decreased signal.

Finally, the blue spectrum in Figure 1A shows the complete P3HT CPB film, with peaks due to S in the thiophene moiety observed at 164.1 eV (S 2p) and 228.0 eV (S 2s). Note that as the P3HT film is sufficiently thick, the N peak is near the detection limit of the instrument and the Si and O peaks are greatly diminished as the mean free path of the XPS generated electrons is exceeded with the APTES templating layers and the polymer film on top of the substrate. Figure 1E shows the C 1s region for the P3HT films which we have fitted with two peaks at 284.8 eV (58.5% peak area) and 286.2 eV (41.5% peak area). These peaks are assigned to the C—C bonding in the polymer and the C—S bond in the thiophene moiety, respectively. The peak shapes and binding energies for the C 1s regions of the **4BB SAM** (Figure 1B), the Pd complex surface (Figure 1D) and the P3HT film (Figure 1E) show the evolution of the carbon bonding present with each subsequent reaction step and the final P3HT film exhibiting a large contribution due to C—S bonding in the thiophene ring. The lack of a Br signal in the P3HT CPB film indicates that disproportionation between Pd-functionalized polymer chain ends may be the mechanism of chain termination, as Pd dissociation prior to oxidative addition to the chain end through a CTP process would leave the terminal thiophene-bromine bond intact, resulting in a bromine signal.[17]

2.3 | Spectroscopic ellipsometry

Table 2 shows the thickness and optical properties of each reaction layer measured by SE except for the Pd catalyst step that were monitored in the XPS experiment with samples that were prepared at the same time for XPS, SE, AFM and contact angle analysis. The Pd step rapidly oxidizes and was impractical to prepare in a glovebox and then perform SE at another location. The thickness measured by ellipsometry of the APTES layer indicates that this is not a monolayer but is actually a multilayer film.[26] It has been shown that APTES can form zwitterions in solution and at film surfaces due to favorable head-to-tail group interactions resulting in multilayer APTES films.[34,35] A single layer APTES film would be expected to have a thickness of 0.7 nm.[27] Ellipsometry indicates that the thickness of the P3HT film is approximately 10 nm, which is consistent with results obtained through scratch profilometry. This value is thinner than the 40–70 nm[16] and 100–200 nm[32] values that have been reported for P3HT CPB films grown with Ni catalysts from cross-linked polystyrene films, but it is thicker than other attempts to grow P3HT CPB films directly from functionalized surfaces.[17]

2.4 | Atomic force microscopy

In a similar manner, AFM data was taken for the APTES, 4BB and P3HT films after each reaction step and are shown in Figure 2. The z-range of the APTES and 4BB layers were 2.0 nm for Figure 2A,B. Both surfaces are flat and uniform with relatively few features. The RMS surface roughness of the APTES film (Figure 2A) is 0.22 nm while the RMS roughness of the 4BB film is 0.51 nm (Figure 2B). The low surface roughness of both of these films is comparable to the regime that Howarter and Youngblood have termed "smooth but thick" APTES films. This would suggest that despite the fact that there is not a monolayer of APTES, the resulting surface would have a uniform ATS enabling further chemical processing. The P3HT film (Figure 2C) is shown with a 10 nm z-range and exhibits an increased RMS surface roughness of 2.45 nm. It exhibits periodic columnar peaks roughly 50 nm in size, which is consistent with the morphology reported in prior literature for P3MT on indium tin oxide.[1] Imaging of the sample shown in Figure 2C at a higher resolution (1.5 × 1.5 μm) provides a clearer view of these columnar peaks (Figure S12).

2.5 | UV–visible spectrophotometry

The optical properties of the CPB film were analyzed via UV–vis spectroscopy by preparing the CPB films on optically transparent glass microscope slides by a similar method to what was described above for oxidized silicon wafers. The P3HT CPB film has a λ_{max} value of

TABLE 2 Spectroscopic ellipsometry calculated refractive index and film thickness.

Layer	Refractive index (*n*)	Calculated thickness (*d*) (nm)	Mean square error (MSE)
Thermal SiO_2 on Si	1.465	99.0	3.1
APTES on SiO_2	1.40	6.5	4.0
4BB SAM	1.40	3.8	1.5
P3HT	1.64	9.0	4.4

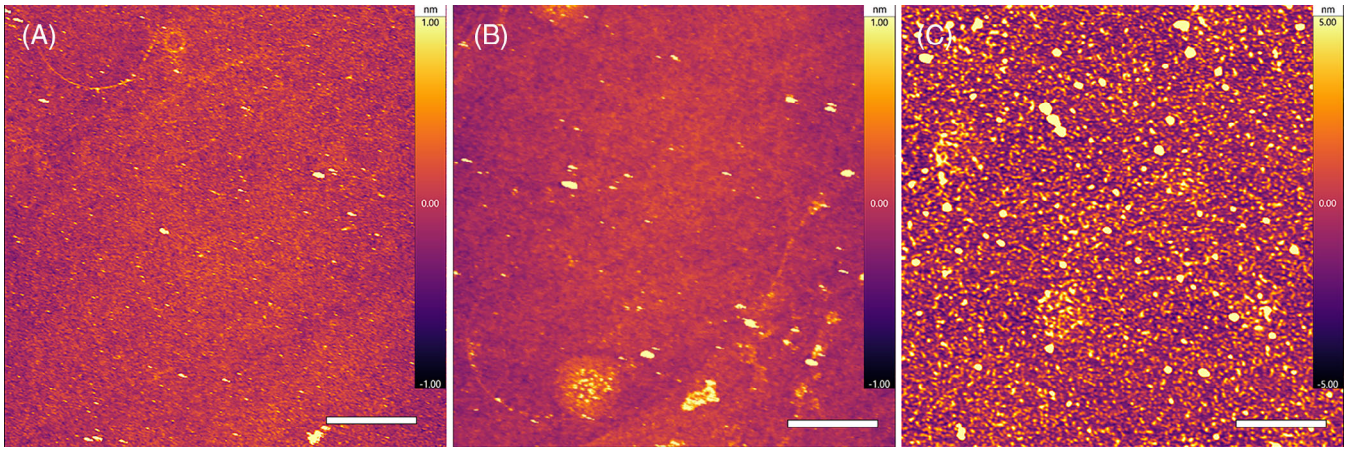

FIGURE 2 10 × 10 μm atomic force microscopy images of (A) (3-aminopropyl)triethoxysilane (APTES)-treated Si/SiO_2 (2.0 nm z-range); (B) 4BB reacted with APTES (2.0 nm z-range); (C) poly(3-hexylthiophene) (P3HT) conjugated polymer brush (CPB) film polymerized from 4BB/Pd terminated surface (10.0 nm z-range). Scale bar = 2 μm for all images.

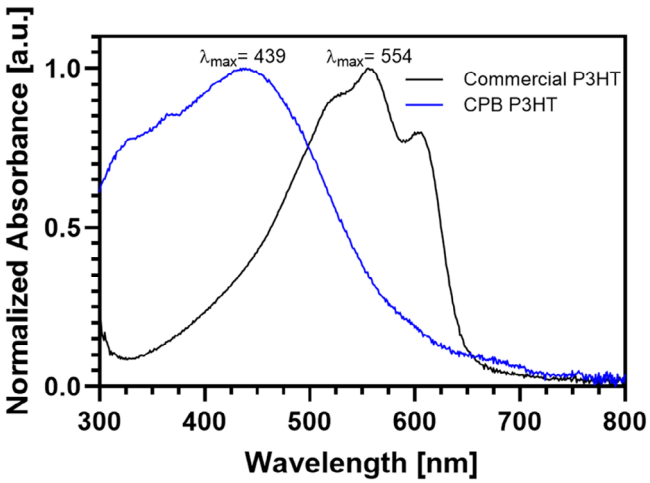

FIGURE 3 UV–vis spectra of poly(3-hexylthiophene) (P3HT) conjugated polymer brush (CPB) films of polythiophene after immersion in chloroform. Data has been baseline corrected in the non-absorbing region of 800 nm and normalized.

442 nm (Figure 3, blue trace), which is consistent with that reported for surface-grafted P3HT[16] and poly(3-methylthiophene) (P3MT).[1,13] This indicates that our method generates CPB films of similar quality to those reported in the literature and underscores the utility of our straightforward method of preparing ATSs capable of initiating CPB film growth for further applications. This λ_{max} value is blue-shifted compared to non-grafted P3HT films drop cast from solution (Figure 3, black trace), indicating that the P3HT CPB exhibits shorter conjugation lengths along its polymer backbone than non-grafted P3HT, perhaps due to greater conformational freedom, which impacts its aggregation behavior.

2.6 | Alternative SAM and polymer preparations

After successfully demonstrating the growth of P3HT films on SiO_2 from an APTES-functionalized surface, we were interested to see how modifications to the ATS preparation procedure would impact the production of our P3HT CPB films. We investigated creating the 4BB surface modification using pre-synthesized 4-bromo-*N*-(3-(triethoxysilyl)propyl)benzamide in a synthesis-first approach (Scheme 3A) as well as using 11-aminoundecyltriethoxysilane AUTES), an analog of APTES with a longer alkyl chain (Scheme 3B). The resulting CPB films were characterized by AFM (Figure 4). The P3HT CPB film morphology is similar for all three ATS preparation methods and structures, indicating that CPB polymerization from all three methods resulted in comparable polymer films. These films also show similar morphology to those reported in the literature,[16] as well as literature reports of polythiophene[3] and P3MT,[1,13–15,18] taking into account that most P3MT CPB films were grown on ITO with only one report on silicon oxide.[13] The surface RMS roughness is comparable for all three films with the original preparation of the P3HT CPB film shown in Scheme 2 having RMS roughness of 2.91 nm (Figure 4A), the 4-bromo-*N*-(3-(triethoxysilyl)propyl)benzamide-derived P3HT CPB shown in Scheme 3A having RMS roughness of 2.15 nm (Figure 4B) and the AUTES-derived P3HT CPB shown in Scheme 3B having RMS roughness of 2.54 nm (Figure 4C). Because the P3HT CPB brush film morphologies are similar, the ATS-first approach with APTES as the precursor is the preferred method, as it does not require rigorous purification of the precursor as in the synthesis-first approach, and APTES can be obtained in much larger quantities at lower cost than the longer chain AUTES.

Poly(3-dodecylthiophene) (P3DDT) films grown using 2-bromo-3-dodecyl-5-iodothiophene as the monomer precursor and the ATS-first preparation with APTES shown in Scheme 2 produce films with a similar morphology to all of the P3HT CPB films and have comparable contact angles. The RMS roughness of the P3DDT film was 1.81 nm (Figure 4D) and the water contact angle = 99.0 ± 3.0° which is similar to all three different types of P3HT CPB films we have prepared. Figure S13 shows a ~30 nm thick P3DDT film polymerized for ~19 h starting from an ATS-first surface on SiO_2. It should be noted that the film thickness measured by scratch cross-section is the total layer thickness including the P3DDT film as well as the underlying 4BB and APTES layers. Based on the ellipsometry data from the P3HT films in Table 2, the P3DDT film is estimated to be ~20 nm thick. This result indicates that the described methodology can be used even with more sterically demanding monomer structures, illustrating the potential of this surface functionalization preparation method for further exploring the structural parameter space of CPB films.

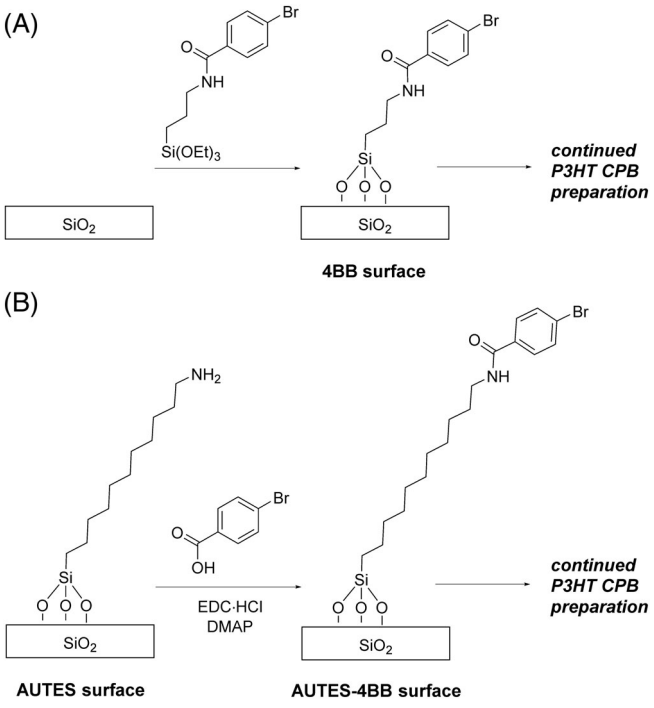

SCHEME 3 Alternative amine-terminated surface (ATS) preparations using: (A) pre-synthesized 4-bromo-*N*-(3-(triethoxysilyl)propyl)benzamide to create the 4BB surface and (B) (11-aminoundecyl)triethoxysilane (AUTES) in place of (3-aminopropyl)triethoxysilane (APTES).

2.7 | P3HT polymerization on Au substrates

We have also applied our strategy for functionalizing planar substrates of gold surfaces using 4-bromo-*N*-(2-mercaptoethyl)benzamide, which was pre-synthesized from 2-aminoethanethiol and 4-bromobenzoic acid using

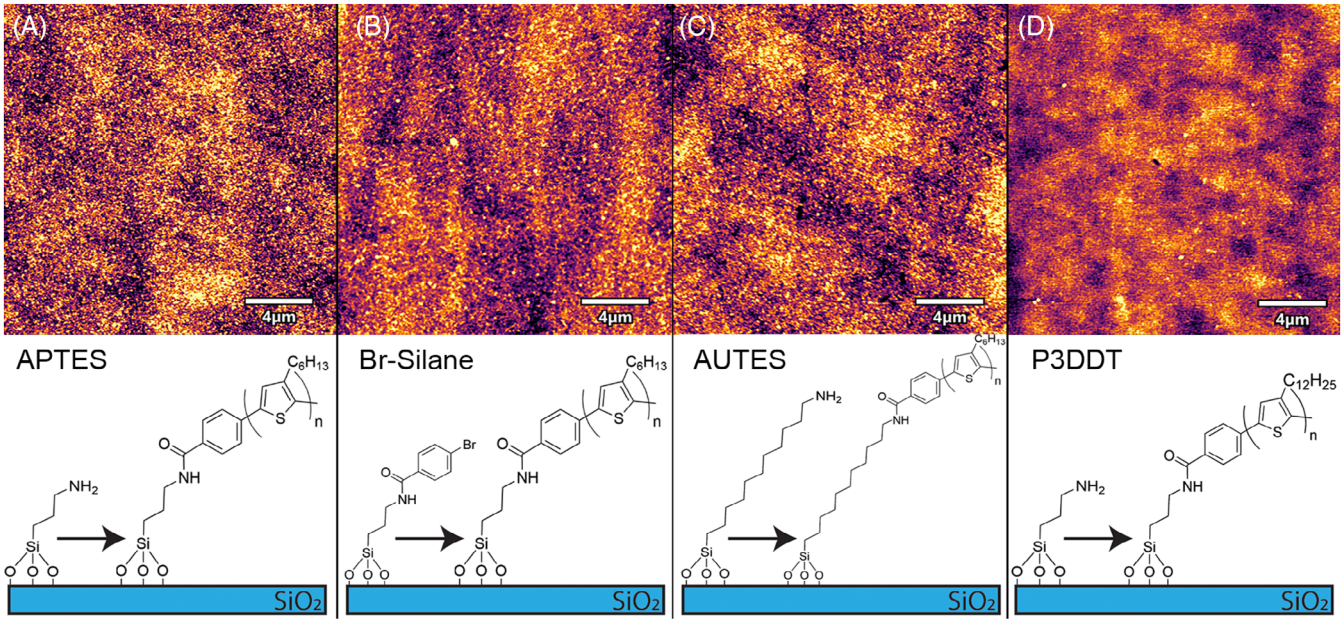

FIGURE 4 20 × 20 μm atomic force microscopy images of poly(3-hexylthiophene) (P3HT) conjugated polymer brush (CPB) films grown from (A) the original preparation from Scheme 2; (B) the synthesized bromine-terminated silane preparation from Scheme 3A; (C) the preparation from (11-aminoundecyl)triethoxysilane (AUTES) from Scheme 3B; (D) analogous film of P3DDT CPB prepared from Scheme 2. All images have a z-scale = 10.0 nm.

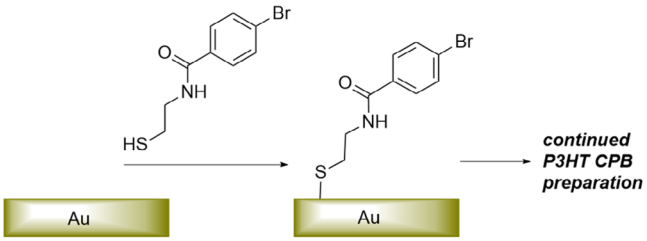

SCHEME 4 Preparation of the surface functionalization on Au for initiating poly(3-hexylthiophene) (P3HT) conjugated polymer brush (CPB) film formation.

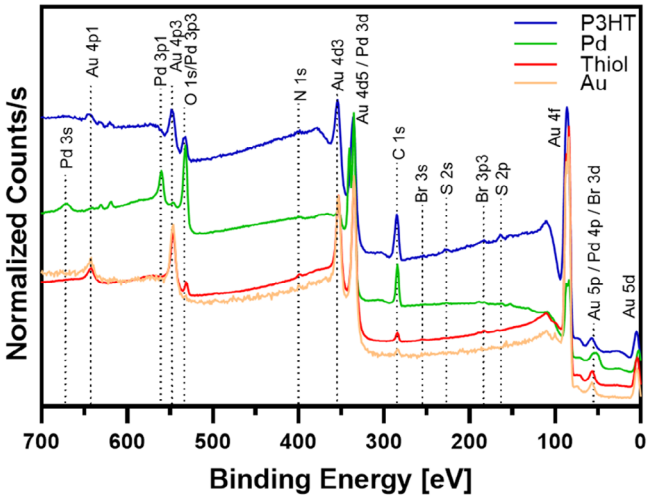

FIGURE 5 X-ray photoelectron spectroscopy (XPS) survey scan from 0 to 700 eV of Au/Cr/Si substrate (gold), synthesized thiol-treated Au film (red), Pd-functionalized surface (green), poly(3-hexylthiophene) (P3HT) grown by catalyst-transfer polycondensation (CTP) (blue). All spectra are normalized to the Au 4f peak and charge compensated to the C 1s peak at 284.8 eV.

peptide coupling reagents, as the initial surface modification layer, as shown in Scheme 4. The quality of ATSs of 2-aminoethanethiol (also known as cysteamine) can be sensitive to concentration and incubation time due to the amine and thiol moieties competing for binding on the Au surface.[36,37] For this reason, the synthesis-first route was chosen for this amine-termination preparation. The Au substrate is immersed in a 1 mM ethanolic solution of the synthesized ATS solution for 24 h followed by a reaction with the Pd complex and then the same P3HT synthesis previously described. XPS survey scans from 0 to 700 eV normalized to the Au 4f peak of each of these reaction steps are shown in Figure 5 and Table 3 has summary atomic concentrations. Unfortunately, the XPS data is not as clean as Figure 1 because there are several cases of peak overlap between the many strong Au peaks and both Pd and Br peaks, but each unique chemical signature can be seen in the four survey spectra in Figure 5

TABLE 3 X-ray photoelectron spectroscopy (XPS) elemental atomic percentages as measured by XPS of each reaction layer starting with an Au substrate.

	Surface termination layer			
Element	**Au**	**Thiol SAM**	**Pd**	**P3HT**
Br 3d	–	2.56	–	–
Au 4f	70.93	47.6	4.47	17.26
S 2p	–	0.45	0.88	2.96
C 1s	25.19	30.03	45.33	68.25
Pd 3d 5/2	–	–	7.44	–
N 1s	–	9.22	1.65	–
O 1s	3.88	10.15	40.23	11.53

and the high-resolution scans in Figures S9–S11. The Au substrate spectrum (gold color) exhibits multiple peaks as labeled due to Au photoelectrons for the 5d, 5p, 4f, 4d 5/2 and 4d 3/2 and 4p and a small peak due to adventitious C in the 0–700 eV binding energy range. The reaction of the thiol ATS layer from Scheme 4 (red spectrum) results in new peaks due to Br 3p 3/2 at 183.3 eV, and 3s at 258.8 eV, a N 1s peak at 399.2 eV, the C 1s peak at 284.9 eV and an O 1s peak at 532.2 eV. There is a small Br 3d peak at 70.4 eV that is close in binding energy with the Au 5p peak at ~73 eV (Figure S9). The reaction with the Pd complex (green spectrum) results in Pd peaks due to Pd 3d (overlapping Au 4d 5/2) at ~335 eV, Pd 3p 3/2 (overlapping O 1s at ~532 eV) and a strong Pd 3p 1/2 peak at 560.7 eV. The lack of a Br signal after Pd insertion yet successful subsequent polymerization implies disproportionation is occurring between Pd-functionalized head groups to a bisaryl Pd(II) complex.[15] Finally, after the CTP reaction to form P3HT (blue spectrum), there are new S peaks due to the 2p and 2s electrons at 163.9 and 228 eV and the C 1s peak is much more prominent as the polymer layer is thicker. Figures S9–S11 and Tables S8–S11 have binding energies, atomic percentages, and high-resolution scans for each element.

2.8 | Patterning of P3HT films using microcontact printing

The ease of μCP on Au surfaces lends itself to soft-lithographic patterning to showcase the utility of our method as a proof of concept.[38] Using a PDMS stamp with 20 μm pitch features, eicosanethiol (ECT) SAM was microcontact printed onto the Au surface in order to pre-pattern the Au substrate with dense hydrophobic methyl-terminated regions which would prevent the functionalized thiol in Scheme 4 from reacting in the ECT printed regions. The ECT

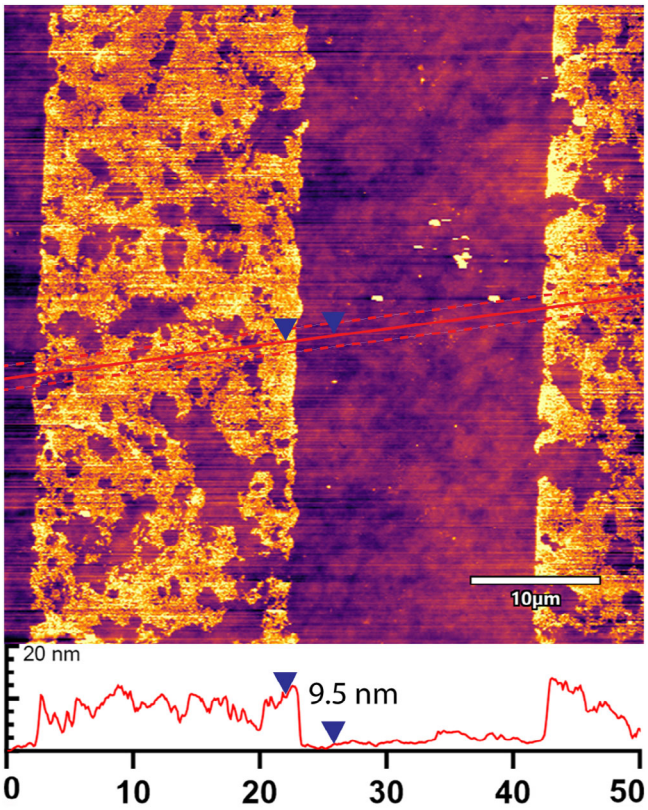

FIGURE 6 50 × 50 μm atomic force microscopy image of poly(3-hexylthiophene) (P3HT) conjugated polymer brush (CPB) films grown from a Au surface patterned using microcontact printing (μCP) of eicosanethiol (ECT) and backfilled with P3HT CPB grafted polymer. Cross-section taking 2.0 μm average as indicated on image with the dashed lines. Measured step height is 9.5 nm. *Z*-scale = 20.0 nm.

pre-printed Au substrate was then immersed in a 2 mM ethanolic solution of 4-bromo-*N*-(2-mercaptoethyl)benzamide for 72 h. Pd-functionalization and polymerization were performed as described previously. The resulting AFM image (Figure 6) shows the distinct regions of the ECT patterned stripe (darker regions) and the surrounding P3HT CPB polymer. The P3HT CPB film morphology grown from the Au surface is consistent with that observed for the SiO_2 surfaces above, although the crystalline domains appear smaller and there are relatively large defects most likely due to the μCP process in our laboratory. Also shown on Figure 6 is a cross-section of the resulting CPB polymer film resulting in ~10 nm thick P3HT layers above the ECT background which is consistent with the film thickness measured by SE (Table 2). We have not explored the full range of μCP parameters such as minimum feature size, ultimate edge resolution/fidelity, different masking thiol SAM layers, etc. although this proof of concept suggests further studies of patterning P3HT CPB films using soft lithography techniques are needed.

3 | CONCLUSION

In conclusion, we have shown that amine-terminated alkylsilanes and -thiols can be coupled to aryl halide-containing carboxylic acids using traditional peptide coupling reagents to produce functionalized surfaces capable of initiating polymerization to produce P3HT CPB films on SiO_2 and Au surfaces, respectively. XPS, AFM, and SE evidence support the surface chemistry and identity throughout all stages of the P3HT CPB film formation, and UV–vis spectrophotometry data suggests, as other studies have in the past, that the conjugation lengths of the polymer chains in these CPB films differ from their non-grafted counterparts. The ATS formation and peptide coupling steps are interchangeable for APTES on Si/SiO_2, as the order does not impact the morphology of the CPB films. However, because the handling of the air-sensitive silane functional group can make purification by column chromatography difficult, it is procedurally easier to form the ATS first and perform the peptide coupling second. Longer amine-terminated alkylsilanes such as AUTES can also be used with minimal impact on film morphology. We have focused on the growth of P3HT CPB films in this report demonstrating for the first time that P3HT (as opposed to P3MT and polythiophene) can be grown from a functionalized surface rather than a cross-linked film of poly(4-bromostyrene), and this method is capable of producing CPB films of the more sterically demanding P3DDT, the first such report to our knowledge. Using a synthesis-first approach with 2-aminoethanethiol, this methodology of P3HT CPB film formation is extended to Au surfaces, and microcontact printing to is used to pattern 20 μm stripes of P3HT CPB. Because our method of producing templating ATSs only requires inexpensive, commercially available reagents that are easily obtained in large quantities, this is an exciting opportunity to expand the structural library of CPB films for applications in polymer-based organic electronics.

4 | EXPERIMENTAL SECTION

4.1 | Materials

(3-Aminopropyl)triethoxysilane (APTES) was obtained from Aldrich, and 11-aminoundecyltriethoxysilane (AUTES) was obtained from Gelest; both reagents were stored in a nitrogen-filled glovebox and used without further purification. A 2.0 M solution of isopropyl magnesium chloride was obtained from Acros, stored in a desiccator, and titrated prior to use.[33] The following reagents were obtained from the vendors indicated and used without further purification:

4-bromobenzoic acid (Oakwood), *N*-(3-dimethylaminopropyl)-*N*′-ethylcarbodiimide hydrochloride (Oakwood), 4-dimethylaminopyridine (Oakwood), bis(tri-*tert*-butylphosphine)palladium(0) (Thermo Scientific), 2-aminoethane thiol (TCI), 4-bromobenzyl mercaptan (Alfa Aesar), eicosanethiol (Thermo Scientific), anhydrous tetrahydrofuran (Acros), anhydrous toluene (Acros), anhydrous acetone (Acros), dichloromethane (BDH), methanol (EMD Millipore), silica gel (Sorbtech). 100 nm thick Au films with a 5 nm Cr adhesion layer were deposited via e-beam evaporation onto Si wafers (100 mm [100], oriented, p-type [1–10 Ω cm] [Virginia Semiconductor]). 100 nm thick SiO_2 films were thermally grown on Si wafers (100 mm, [100], oriented, p-type [1–10 Ω cm] [Virginia Semiconductor]). Dow Sylgard 184 curing agent and resin were used to produce polydimethylsiloxane (PDMS) elastomeric microcontact printing masters.

4.2 | General synthetic considerations

Synthetic procedures were performed under inert atmosphere unless otherwise noted. Column chromatography was performed using a Biotage Selekt or a Teledyne Combiflash NextGen 300+. NMR spectra were recorded using a JEOL ECZ-400S NMR spectrometer. Small-molecule mass spectrometry was performed on a Shimadzu GCMS-QP2020NX gas chromatography-mass spectrometer.

4.3 | Synthesis of 4-bromo-*N*-(3-(triethoxysilyl)propyl)benzamide

In a nitrogen-filled glovebox, 4-bromobenzoic acid (1.208 g, 6.00 mmol), (3-aminopropyl)triethoxysilane (APTES) (1.6 mL, 6.8 mmol, 1.1 equiv), *N*-(3-dimethylaminopropyl)-*N*′-ethylcarbodiimide hydrochloride (EDC·HCl) (1.376 g, 7.18 mmol, 1.2 equiv), 4-dimethylaminopyridine (DMAP) (0.073 g, 0.60 mmol, 0.10 equiv), and anhydrous dichloromethane (30 mL) were added to a round bottom flask. The flask was capped with a rubber septum, and the reaction was allowed to stir at room temperature overnight. The flask was brought out of the glovebox and the solution was filtered through a canula with a filter paper wired onto the end and transferred to a round bottom flask under nitrogen. The following steps were performed with minimal delay in air to avoid polymerization: the solution was concentrated with rotary evaporation, and the residue was purified by column chromatography in 15%–35% ethyl acetate in hexanes to afford the product as a colorless waxy solid (1.328 g 3.28 mmol, 54.7% yield). ^{1}H NMR (400 MHz, $CDCl_3$ δ): 7.70–7.62 (m, 2H; Ar H), 7.60–7.52 (m, 2H; Ar H), 6.54 (s, 1H; NH), 3.83 (q, $J = 7.0$ Hz, 6H; OCH_2), 3.46 (q, $J = 6.5$ Hz, 2H; CH_2), 1.75 (dq, $J = 8.2$, 6.9 Hz, 2H; CH_2), 1.22 (t, $J = 7.0$ Hz, 9H; CH_3), 0.81–0.62 (m, 2H; $SiCH_2$). ^{13}C NMR (101 MHz, $CDCl_3$, δ): 166.61 (C═O), 133.91 (C—C═O), 131.84 (*m*-C), 128.69 (*o*-C), 126.02 (C-Br) 58.71 (C—O), 42.36 (C3), 22.94 (C2), 18.44 (CH_3), 7.99 (C1). EIMS m/z (%): 403.1 (2) [M^+], 405.1 (2) [M^++2], 357.1 (45) [M^+ − EtOH], 359.1 (47) [M^++ − EtOH], 163.1 (100) [$(EtO)_3Si^+$].

4.4 | Synthesis of 4-bromo-*N*-(2-mercaptoethyl)benzamide

An oven-dried, three-neck round bottom flask attached to a Schlenk line was charged with 2-aminoethanethiol (375 mg, 4.86 mmol), 4-bromobenzoic acid (1.10 g, 5.47 mmol, 1.12 equiv), EDC·HCl (1.15 g, 6.00 mmol, 1.23 equiv), and DMAP (107 mg, 0.876 mmol, 0.180 equiv), and the flask was vacuum-purged with nitrogen three times. To the flask was added anhydrous dichloromethane (25 mL). The reaction was allowed to stir at room temperature overnight. The precipitate was removed by vacuum filtration and the solution was concentrated. The residue was purified by column chromatography in 10%–60% ethyl acetate in hexanes to afford the product as a white solid (185 mg, 0.711 mmol, 14.6% yield). ^{1}H NMR (400 MHz, $CDCl_3$, δ): 7.69–7.63 (m, 2H; Ar H), 7.61–7.55 (m, 2H; Ar H), 6.54 (s, 1H; NH), 3.76–3.55 (m, 2H; NCH_2), 2.80 (dt, $J = 8.4$, 6.3 Hz, 2H; SCH_2), 1.40 (t, $J = 8.5$ Hz, 1H; SH). ^{13}C NMR (101 MHz, $CDCl_3$, δ): 166.68 (C═O), 133.23 (C—C═O), 132.03 (*m*-C), 128.70 (*o*-C), 126.51 (C—Br), 42.86 (C2), 24.87 (C1); EIMS m/z (%): 259.1 (5) [M^+], 261.1 (5) [M^++2], 155.0 (16) [$C_6H_4Br^+$], 157.0 (17) [$C_6H_4Br^+$+2], 183.0 (52) [M^+ − $HSCH_2CH_2NH$], 185.0 (52) [M^++2 − $HSCH_2CH_2NH$].

4.5 | Bromine-terminated surface preparation on oxidized silicon wafers and glass coverslips (general procedure)

Oxidized silicon wafers and glass coverslips were cut and sonicated for 5 min sequentially in acetone, isopropyl alcohol, and 18 MΩ cm MilliQ water and dried with compressed nitrogen after every sonication step. The samples were subjected to O_2 plasma cleaning for 2 min and then submerged in 2% v/v solution of the respective silane (APTES or AUTES) in anhydrous acetone for 30 min. They were removed, rinsed with acetone and oven dried for 5 min at 80°C.

The substrates were then submerged in a solution of 1.27 g (6.32 mmol) 4-bromobenzoic acid, 1.38 g

(7.20 mmol) EDC·HCl, and 72 mg (0.59 mmol) DMAP in 30 mL dichloromethane and left at room temperature overnight. The substrates were removed, rinsed with dichloromethane and dried.

4.6 | ATS preparation on silicon wafers and glass coverslips

Oxidized silicon wafers and glass coverslips were cut and sonicated for 5 min sequentially in acetone, isopropyl alcohol, and 18 MΩ cm MilliQ water and dried with compressed nitrogen after every sonication step. The samples were subjected to O_2 plasma cleaning for 2 min and then submerged in 2% v/v solution of the respective silane (APTES or AUTES) in anhydrous acetone for 30 min. They were removed, rinsed with acetone and oven dried for 5 min at 80°C. The substrates were submerged in a 10% v/v solution of 4-bromo-*N*-(3-(triethoxysilyl)propyl)benzamide in anhydrous acetone for 30 min. They were removed, rinsed with acetone and oven dried for 5 min.

4.7 | Palladium-functionalization and surface-initiated polymerization of P3HT (general procedure)

In a nitrogen-filled glovebox, the substrates were submerged in a 10 mM $Pd(P\textit{t}\text{-}Bu_3)_2$ solution in toluene for 3 h at 70°C.

Meanwhile, in the reaction hood equipped with a Schlenk line, the isopropyl magnesium chloride solution was titrated with I_2 in a THF solution of LiCl immediately before polymerization set-up.[33] The average concentration of three trials was used. A solution of 0.05 M monomer was then generated by charging an oven-dried, vacuum-purged 20-mL vial with a septum cap with 0.1872 g (0.5018 mmol) of 2-bromo-3-hexyl-5-iodothiophene and 10 mL of anhydrous THF. The monomer solution was cooled to 0 °C and 0.96 equiv of recently titrated iPrMgCl in THF was added. The reaction was allowed to stir at 0 °C for 1 h and then the vial was transferred into the glovebox.

The substrates were removed from the Pd solution, rinsed with toluene and submerged in the monomer solution for 22 h at room temperature inside the glovebox. The substrate was then removed from solution and quenched in methanol and transferred outside of the glovebox. The substrates were then sonicated sequentially in chloroform, acetone, methanol, and water for 5 min each, and then dried with compressed nitrogen.

4.8 | Microcontact printing

All microfabricated structures used for μCP master fabrication were prepared in a Class 100 cleanroom using SU-8 negative photoresist (Kayaku SU-8 2) and exposed using a OAI 8808 mask aligner through a custom designed 5‴ Cr/glass mask resulting in a repeating pattern of 20 μm lines and spaces. The SU-8 resist was spun-cast at 2000 rpm resulting in a thickness ∼2 μm. After exposure samples were developed in isopropyl alcohol for 60 s. 3 × 3 cm samples were cleaved from the patterned Si substrates in preparation for PDMS master production. Sylgard 184 resin and curing agent were mixed in a 10:1 ratio by mass in accordance with manufacturer's instructions, degassed in a vacuum oven at room temperature to remove any residual air bubbles resulting from the mixing process, poured onto the SU-8/Si master, and cured in an oven at 100°C for 1 h at atmospheric pressure.

Gold-coated wafers were sonicated for 5 min and dried with compressed nitrogen sequentially in acetone, isopropyl alcohol and 18 MΩ cm MilliQ water. Cleaned samples were then sputter coated with gold for 20 s using a Cressington 108 sputter coater with a quartz crystal thickness monitor to ensure that the Au-coated wafers had ∼5 nm of new Au immediately prior to alkanethiol SAM deposition. The PDMS stamp was covered with a 0.2 mM solution of eicosanethiol (ECT) in anhydrous ethanol by dropping with a micropipette at a volume of 1 μL/mm^2 stamp. The drop was removed after 30 s using a stream of compressed nitrogen which was continued for an additional ∼10 s following the procedure described by Delamarche, et al.[38] The stamp was placed on the Au surface for 30 s under its own weight then removed. The substrate was rinsed with ethanol and dried with compressed nitrogen. The substrate was then placed in a 2 mM solution of 4-bromo-*N*-(2-mercaptoethyl)benzamide in ethanol for 72 h. The substrates were then rinsed with ethanol and dried with compressed nitrogen. They were then transferred into the glovebox, where they were palladium functionalized and used for surface-initiated polymerization of P3HT CPB films as described above.

4.9 | Materials characterization

The materials and chemical properties of the chemically modified surfaces and P3HT films were characterized by AFM, SE, contact angles and XPS. All samples were imaged with AC mode AFM using an Asylum Research MFP-3D Origin+ instrument. Standard Al coated Si tapping mode probes were used having a resonance frequency ∼300 kHz and a spring constant, $k = 26$ N/m. (Olympus OMCL-AC160). All imaging was performed in

air, and images were collected at a resolution of 512 × 512 pixels with varying scan-ranges as noted. Any scan line errors were removed, a software mask was applied to pixels that were significantly higher than the resulting film and a first order flatten was performed on each sample to remove scan artifacts. Roughness measurements and cross-section analysis were performed after flattening. Scratch cross-section analysis was performed on the P3DDT films by scratching the polymer surface with a new razor blade.

UV–visible spectroscopy was performed on a Cary 3000 UV–visible spectrophotometer. Thin films of commercial P3HT (Aldrich) dissolved in chloroform were drop-cast onto microscope slides and the solvent was allowed to evaporate leaving a cast film. P3HT CPB films were produced as described above using the APTES ATS on microscope cover slides to compare transmission UV–vis spectra from each film type from 300 to 800 nm.

Optical properties and thickness of the various SAM templating layers and the P3HT CPB films grafted from SiO_2/Si substrates were measured using a J.A. Wollam variable angle spectroscopic ellipsometer (VASE) instrument at a fixed angle of incidence of 70°. Based on UV–vis spectroscopy, each of the layers except for the P3HT were assumed to be non-absorbing through the visible and near-IR range, so the SiO_2, APTES and bromobenzene films were fitted from 400 to 1000 nm while the P3HT film was analyzed from 550 to 1000 nm in a non-absorbing region. The optical properties for thermal SiO_2 and crystalline Si are well-known and were used for the substrate calculation.[39] Since the optical properties of the subsequent films are not known, a non-absorbing Cauchy film from 400 to 1000 nm was assumed for both the APTES and the 4BB layers starting with an initial refractive index $n = 1.4$ and then both index and thickness were optimized. An index of 1.4 was chosen for the ATPES and 4BB films as an initial starting point because this is a typical refractive index of organic films through the visible spectral region. Once the mean square error was minimized for each reaction step, the model fitting parameters (n and d) were fixed in the software for that film layer in order to calculate the subsequent film layer, thus building up an optical model for the SE characterization layer by layer.

Static water contact angle measurements were performed with a Biolin Scientific Theta Lite Optical Tensiometer using 18 MΩ cm MilliQ deionized H_2O and a manual syringe to dispense a drop with a volume of 1.5 μL in order to measure the sessile drop static contact angle. Five H_2O drops were measured on each surface type on the right and left side of each drop. Measurements were taken every 0.1 s for 10 s totaling 200 measurements per drop (100 right and left) and then measurements from all five drops were averaged. The Pd catalyzed surface was not measured using contact angles due to the relatively rapid oxidation of the Pd catalyst surface.

X-ray photoelectron spectroscopy (XPS) was performed using a Thermo Scientific ESCALAB Xi+ instrument using an Al K-alpha source (1486.2 eV) having a microfocusing monochrometer and a hemispherical analyzer. Survey scans ($N = 25$) of each of the films were taken from 0 to 1350 eV binding energy. Elemental scans ($N = 30$) of each of the major element peaks were performed with a pass energy of 30 eV. All spectra were charge compensated to the adventitious C 1s peak at 284.8 eV. XPS survey spectra binding energies were assigned by the instrument software and high-resolution elemental XPS peaks were assigned based on literature values reported in the NIST X-ray Photoelectron Spectroscopy Database (SRD 20), Version 5.0.[40]

ACKNOWLEDGMENTS

This research was supported through the National Science Foundation Major Research Instrumentation Program (1919685 and 2320222), the North Carolina Biotechnology Center (2023-FLG-0025), the National Science Foundation National Nanotechnology Coordinated Infrastructure program (ECCS-20254P62 and ECCS-2025064), and High Point University. The manuscript was written with contributions from all authors. Synthesis, AFM, UV–vis spectroscopy, μCP, and contact angle measurements were performed by Olivia J. Armendarez, Grace C. Parizek, Ruth J. Augustine, Evan J. Silver, Tristan A. Kaz, Kaylee A. Campbell, Isabella P. Diaz, Shobha Mantripragada. XPS was performed by Shobha Mantripragada and SE was performed by Robert D. Geil. The experimental design, planning, data analysis and manuscript preparation were conducted by Brian H. Augustine and Pamela M. Lundin. All authors have given approval to the final version of the manuscript.

ORCID

Olivia J. Armendarez https://orcid.org/0009-0007-8323-0352
Grace C. Parizek https://orcid.org/0000-0003-3055-4429
Ruth J. Augustine https://orcid.org/0009-0001-0182-9537
Kaylee A. Campbell https://orcid.org/0009-0005-9462-0183
Isabella P. Diaz https://orcid.org/0009-0004-1358-2705
Shobha Mantripragada https://orcid.org/0000-0002-9735-7246
Sadie M. Flagg https://orcid.org/0009-0006-9435-0192
Brian H. Augustine https://orcid.org/0000-0003-2115-911X

Pamela M. Lundin https://orcid.org/0000-0002-6071-1440

REFERENCES

[1] I. A. VonWald, M. M. Moog, T. W. LaJoie, J. D. Yablonski, D. M. DeLongchamp, J. Locklin, F. Tsui, W. You, *J. Phys. Chem. C* **2018**, *122*, 7586.
[2] A. Roy, T. L. Bougher, R. Geng, Y. Ke, J. Locklin, B. A. Cola, *ACS Appl. Mater. Interfaces* **2016**, *8*, 25578.
[3] S. G. Youm, E. Hwang, C. A. Chavez, X. Li, S. Chatterjee, K. L. Lusker, L. Lu, J. Strzalka, J. F. Ankner, Y. Losovyj, J. C. Garno, E. E. Nesterov, *Chem. Mater.* **2016**, *28*, 4787.
[4] L. Yang, S. K. Sontag, T. W. LaJoie, W. Li, N. E. Huddleston, J. Locklin, W. You, *ACS Appl. Mater. Interfaces* **2012**, *4*, 5069.
[5] R. Geng, A. Roy, W. Zhao, R. C. Subedi, X. Li, J. Locklin, T. D. Nguyen, *Adv. Funct. Mater.* **2016**, *26*, 3999.
[6] W. Hou, N.-J. Zhao, D. Meng, J. Tang, Y. Zeng, Y. Wu, Y. Weng, C. Cheng, X. Xu, Y. Li, J.-P. Zhang, Y. Huang, C. W. Bielawski, J. Geng, *ACS Nano* **2016**, *10*, 5189.
[7] M. A. Islam, T. K. Purkait, M. H. Mobarok, I. M. D. Hoehlein, R. Sinelnikov, M. Iqbal, D. Azulay, I. Balberg, O. Millo, B. Rieger, J. G. C. Veinot, *Angew. Chem. Int. Ed.* **2016**, *55*, 7393.
[8] V. Senkovskyy, R. Tkachov, T. Beryozkina, H. Komber, U. Oertel, M. Horecha, V. Bocharova, M. Stamm, S. A. Gevorgyan, F. C. Krebs, A. Kiriy, *J. Am. Chem. Soc.* **2009**, *131*, 16445.
[9] F. Monnaie, L. Verheyen, J. De Winter, P. Gerbaux, W. Brullot, T. Verbiest, G. Koeckelberghs, *Macromolecules* **2015**, *48*, 8752.
[10] D. Meng, S. Yang, L. Guo, G. Li, J. Ge, Y. Huang, C. W. Bielawski, J. Geng, *Chem. Commun.* **2014**, *50*, 14345.
[11] M. A. Baker, C.-H. Tsai, K. J. T. Noonan, *Chem. Eur. J.* **2018**, *24*, 13078.
[12] N. Doubina, S. A. Paniagua, A. V. Soldatova, A. K. Y. Jen, S. R. Marder, C. K. Luscombe, *Macromolecules* **2011**, *44*, 512.
[13] S. K. Sontag, G. R. Sheppard, N. M. Usselman, N. Marshall, J. Locklin, *Langmuir* **2011**, *27*, 12033.
[14] N. Doubina, J. L. Jenkins, S. A. Paniagua, K. A. Mazzio, G. A. MacDonald, A. K.-Y. Jen, N. R. Armstrong, S. R. Marder, C. K. Luscombe, *Langmuir* **1900**, *2012*, 28.
[15] I. A. VonWald, S. G. Frye, M. M. Moog, C. L. Donley, F. Tsui, W. You, *J. Phys. Chem. B* **2020**, *124*, 9734.
[16] V. Senkovskyy, N. Khanduyeva, H. Komber, U. Oertel, M. Stamm, D. Kuckling, A. Kiriy, *J. Am. Chem. Soc.* **2007**, *129*, 6626.
[17] N. Marshall, A. Rodriguez, *PeerJ Mat. Sci.* **2020**, *2*, e6.
[18] N. E. Huddleston, S. K. Sontag, J. A. Bilbrey, G. R. Sheppard, J. Locklin, *Macromol. Rapid Commun.* **2012**, *33*, 2115.
[19] S. K. Sontag, N. Marshall, J. Locklin, *Chem. Commun.* **2009**, 3354. https://doi.org/10.1039/b907264k
[20] S. K. Vashist, E. Lam, S. Hrapovic, K. B. Male, J. H. T. Luong, *Chem. Rev.* **2014**, *114*, 11083.
[21] W. Zhang, E. P. C. Lai, *Silicon* **2022**, *14*, 6535.
[22] N. Bouazizi, J. Vieillard, B. Samir, F. Le Derf, *Polymer* **2022**, *14*, 378.
[23] C. Nicosia, J. Huskens, *Mater. Horiz.* **2014**, *1*, 32.
[24] C. Haensch, S. Hoeppener, U. S. Schubert, *Chem. Soc. Rev.* **2010**, *39*, 2323.
[25] Y. Xia, X.-M. Zhao, G. M. Whitesides, *Microelectron. Eng.* **1996**, *32*, 255.
[26] J. A. Howarter, J. P. Youngblood, *Langmuir* **2006**, *22*, 11142.
[27] A. Zarinwall, T. Waniek, R. Saadat, U. Braun, H. Sturm, G. Garnweitner, *Langmuir* **2021**, *37*, 171.
[28] M. Brinkmann, *J. Polym. Sci. Part B: Polym. Phys.* **2011**, *49*, 1218.
[29] A. Marrocchi, D. Lanari, A. Facchetti, L. Vaccaro, *Energy Environ. Sci.* **2012**, *5*, 8457.
[30] N. E. Persson, P.-H. Chu, M. McBride, M. Grover, E. Reichmanis, *Acc. Chem. Res.* **2017**, *50*, 932.
[31] N. Marshall, S. K. Sontag, J. Locklin, *Chem. Commun.* **2011**, *47*, 5681.
[32] T. Zhang, R. D. Rodriguez, I. Amin, J. Gasiorowski, M. Rahaman, W. Sheng, J. Kalbacova, E. Sheremet, D. R. T. Zahn, R. Jordan, *J. Mater. Chem. C* **2018**, *6*, 4919.
[33] A. Krasovskiy, P. Knochel, *Synthesis* **2006**, *2006*, 890.
[34] W.-Y. Wang, K. Kala, T.-C. Wei, *Langmuir* **2018**, *34*, 13597.
[35] Y. Li, P. Jia, J. Xu, Y. Wu, H. Jiang, Z. Li, *Ind. Eng. Chem. Res.* **2020**, *59*, 2874.
[36] S. Y. Lee, J. Noh, E. Ito, H. Lee, M. Hara, *Jpn. J. Appl. Phys.* **2003**, *42*, 236.
[37] J. Zhang, A. Bilic, J. R. Reimers, N. S. Hush, J. Ulstrup, *J. Phys. Chem. B* **2005**, *109*, 15355.
[38] E. Delamarche, H. Schmid, A. Bietsch, N. B. Larsen, H. Rothuizen, B. Michel, H. Biebuyck, *J. Phys. Chem. B* **1998**, *102*, 3324.
[39] R. Philipp, in *Handbook of Optical Constants of Solids* (Ed: E. D. Palik), San Diego: Elsevier, **1985**, p. 749.
[40] NIST, X-ray photoelectron spectroscopy database, NIST Standard Reference Database Number 20, National Institute of Standards and Technology, 20899. **2000** https://doi.org/10.18434/T4T88K

SUPPORTING INFORMATION

Additional supporting information can be found online in the Supporting Information section at the end of this article.

How to cite this article: O. J. Armendarez, G. C. Parizek, R. J. Augustine, E. J. Silver, T. A. Kaz, K. A. Campbell, I. P. Diaz, S. Mantripragada, R. D. Geil, S. M. Flagg, B. H. Augustine, P. M. Lundin, *J. Polym. Sci.* **2024**, *62*(23), 5384. https://doi.org/10.1002/pol.20240377